An Experimental Study of Aerodynamic Drag on the Body of Road Vehicle

Dr. Vakkar Ali
Department of Mechanical and Industrial Engineering, Majmaah University, K.S.A.

Any moving object through a fluid experiences a force in the direction opposite to the motion which is due to the pressure difference and shear forces on the surface of the object. If we resolve the resultant force in the direction of flow and normal to flow then there are termed as aerodynamic drag force, aerodynamic lift force respectively. If aerodynamic drag acting on the automobiles or aero planes is less, then it will consume a lesser power resulting in less fuel consumption. In the present proposed study we have look after practical aspect of an model of automobile car, (Maruti Esteem). For practical approach, we have to analyze the available model to see the factors, which may reduce drag force on the surface of the moving body. In the present work drag force is calculated on the body of car model experimentally on the basis of our findings drag force is directly proportional to the angle of wind screen, velocity, surface, and fluid viscosity.

Keywords: Aerodynamic drag force, Aerodynamic lift force.

1. INTRODUCTION

Boundary layer flow has been considered for studying the drag force on the surface of model of automobile vehicle. The body of an Automobile is often made by three portions as bonnet, wind screen and roof. The portion facing the driver is being considered as moving plate in a fluid and the portion including the wind screen is taken as a wedge. The influence of automobile velocity and wind screen angle on the drag force is obtained by numerical computation. C.P. Van Dam [1] applied the fluid dynamics (CFD) tool to study and predict the aerodynamic characteristics of vehicle. He reviewed recent experiences in one of the kinds of aerodynamic drag is due to boundary layer flow over the body of an Automobile. In the present work CFD based drag prediction with an emphasis on flow solutions governed by Euler and Reynolds verged Navier-Stokes equations, is given. Aerodynamic drag influences many characteristics of an automobile like fuel consumption, maximum speed and braking characteristics that are directly affected by the aerodynamics [2]. Elena Laurent used the experimental and numerical approach to obtain the efficient development processes for new vehicle drag force due to boundary layer formation depends on the type of flow. It is directly proportional to the Reynolds number. Effect of turbulent wall-bounded flow [3] investigated by Mohammed Gadel Hak in wind tunnel to measure accurate drag. There are many drag acting on the body of an automobile during the movement in a fluid other than the drag due to boundary layer formation wave drag and induced drag. David Nixon carried on a comparative analysis between wave drag and induced drag on the surface of automobile [4]. He investigated that at low velocities the wave drag is much less as induced one.

Therefore, pressure difference and momentum change with respect to time are very small, that produces low value of drag. Similarly D. Destarac and V.J. Vander studied the drag on the jet-propelled aircraft on the basis of viscous flow [5]. In doing so, they divided the total drag into three components, viscous drag, wave drag and induced drag. Analytical and experimental techniques are being used to determine the drag in the present era. Zhan *et al*. studied the effect of the Reynolds number, net solidity, mesh pattern and flow direction on the drag force on the submerged net of fish cages through these techniques [6]. Mathematical exact approaches has used by Pollaniappan and Ramkissoon [7] to investigate the elegant formula for drag. Shao and Yang studied the schema for drag partition over the rough surfaces [8]. They carried forward his studies by dividing the fatal drag in three components, pressure drag, slim drag due to momentum transfer to the surface of rough non element and surface drag due to momentum transfer to the ground surface. Some researcher like Manoj Kumar and S.V. Anantha investigated pressure related drag [9] on numerical modeled ship model. In this study the ship model runs at speed essentially within the range of the laminar and transient flows. The residual resistance values are compared with the numerical result.

None of the referred authors have considered car model of moving automobiles to compute the drag on their effective body position. In the present work we compute the drag on bonnet, wind screen and roof and find the results with the experimental set up by testing the same model on the wind tunnel. In this analysis we have taken Indian make automobile passenger car i.e. Maruti Esteem as shown in Figure 1. The effects of shape size and angel of screen on drag force are computed experimentally.

Fig. 1: Maruti Esteem Car to be tested for Drag force Analysis.

2. FUNCTION OF STRAIN GAUGES

Resistance wire strain gauges are transducers applied to the surface of structural members under test in order to sense the elongation or strain due to applied loads. The wire strain gauges depend upon the fact that when the wire is stretched elastically, its length and diameter are altered. This resulting in overall change of resistance due to both the dimensional changes as:

$$R = \rho \times \frac{L}{A} \quad (1)$$

The resistance of a conductor of length L and area cross-section A is given by eqn (1).

2.1. Strain and displacement measurement

The popularity is mainly due to the fact that they satisfy most of the requirement of an ideal gauge. The basic principle of these strain gauges was known as early as 1856. Two engineers first perfected the bonded wire strain gauge in 1938, almost simultaneously. They were Simmons at California Institute of Technology and Rouge at Massachusetts Institute of Technology in U.S.A.

2.2. Strain sensitivity

It was in 1856 that Lord Kelvin proposed the principle on which today's strain gauges are built and used. Lord Kelvin demonstrated that electrical resistance of certain wires changed with respect to tension to which they were subjected.

Differentiating Equation (1) and divided it by R gives

$$\frac{dR}{R} = \frac{d\rho}{\rho} + \frac{dL}{L} - \frac{dA}{A} \tag{2}$$

Assuming that the wire has been stretched by an axial loading causing on axial strain of $\frac{dL}{L}$, then the term $\frac{dA}{A}$ will represent reduction in area per unit area of x-section due to transverse strain.

Transverse strain = $\frac{d_c - d_0}{d_0} = -\nu \frac{dL}{L}$

Where, d_0 = Original diameter

d_c= Current diameter or diameter after stress is applied

Hence, $d_c = d_0\left(1 - \nu \frac{dL}{L}\right)$

Where ν is Poisson's ratio of material wire,

Hence final area $= \frac{\pi}{4} d_c^2 = \frac{\pi}{4} d_0^2 \left[1 - 2\nu \frac{dL}{L} + \nu^2 \left(\frac{dL}{L}\right)^2\right]$

Final area $= \frac{\pi}{4}\left[-2\nu\, d_0^2 \frac{dL}{L} + \nu^2 \left(d_0 \frac{dL}{L}\right)^2\right]$

Also $$\frac{A_c - A_0}{A_{.0}} = \frac{dA}{A} = \frac{\frac{\pi}{4}\left[-2\nu\, d_0^2 \frac{dL}{L} + \nu^2 \left(d_0 \frac{dL}{L} \right)^2 \right]}{\frac{\pi}{4} d_0^2}$$

Finally, $$\frac{A_c - A_0}{A_{.0}} = -2\nu \frac{dL}{L} + \left(\nu \frac{dL}{L} \right)^2 \quad (3)$$

In equation (3), the second term of RHS is square of $\left(\nu \frac{dL}{L} \right)$ and each of ν and $\frac{dL}{L}$ is very small.

Hence this term can be neglected.

Hence equation (3) reduces to,

$$\frac{dA}{A} = -2\nu \frac{dL}{L} \quad (4)$$

From equation (4) and equation (2), we get

$$\frac{dR}{R} = \frac{d\rho}{\rho} + \frac{dL}{L} + 2\nu \frac{dL}{L} \quad (5)$$

Also the longitudinal strain ($\in$) in the wire is given by

$$\in = \frac{dL}{L} \quad (6)$$

By equation (6), equation (5) reduces to

$$\frac{dR}{R} = \frac{d\rho}{\rho} + \in (1 + 2\nu) \quad (7)$$

Therefore $$\frac{\frac{dR}{R}}{\in} = \frac{\frac{d\rho}{\rho}}{\in} + (1 + 2\nu) \quad (8)$$

The quantity $\frac{\frac{dR}{R}}{\in}$ is defined as the strain sensitivity of the conductor material and is denoted by SA. For most of the materials that are used for making the gauges υ = 0.3, hence factor (1+2υ) =1.6.

2.3. Fixing the Gauges

Before the strain gauge can be used for measurement of strain it has to be intimately cemented on to the surface. The operation of mounting of gauges can be separated into four different stages. Preparation of the surface where the gauge is to be applied is the first step towards gauge installation. Any dirt or oil will not allow the cement to set uniformly. Therefore the surface must be thoroughly cleared of oil, rust, paint or scaling. A fairly liberal layer of cement is spread on the surface of specimen. The side of the gauge that will come in contact with cement must not be touched with fingers and preferably cleaned with cotton swab soaked in organic solvent.

A thin layer of cement may also be applied on the side of gauge. For the purposes of alignment a light line may be inscribed on the specimen surface before application of the cement. The gauge is then placed at the spot making contact with the cement. The gauge is then pressed and rolled lightly with fingers to squeeze out the most of the excess cement. A light weight of about 1/2 kgf may be placed on the top of a rubber pad placed upon the gauge. The curing may be accelerated in some cement by blowing hot air on the metal surface close to the gauge.

A check for perfect drying is to measure the gauge resistance during process of curing. As the gauge cement dries the resistance of the gauge increases and levels off when the gauge is perfectly cured.

2.4. Lead Wire Connection and Testing

Lead wires are selected for low electrical resistance. The wires should have good insulation and flexible in handling. Single core covered with thermoplastic insulation or similar stranded wires are good for room temperature application. Before soldering wire leads, tying them with structure or cementing them near the gauge will eliminate accidental damage to the gauge during soldering. Special connectors placed between the gauge and lead wires are often helpful for this purpose. A schematic diagram of connections is shown in Figure 2.

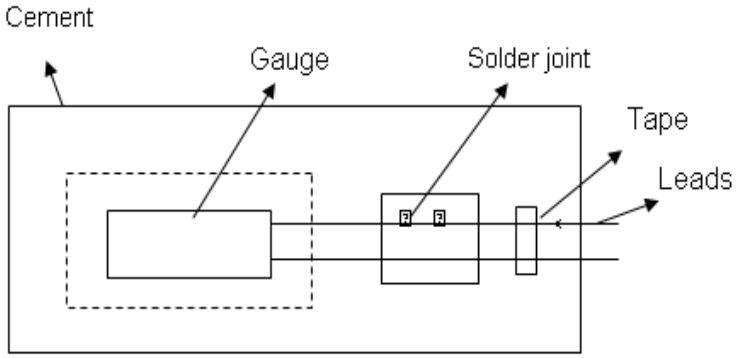

Fig. 2: Strain Gauge with Leads Connection.

2.5. Principle and strain gauge mounting

The forces H (drag) and V (lift) are made to act at the end of a cantilever. Total eight gauges are used to measure the drag and lift force. The four gauges i.e. R1H, R2H, R1V and R3V are pasted on the top face while R3H, R2V, R4V and R4H pasted on the bottom side of the cantilever as shown in Figure 3. Bridge of R1H, R2H, R3H and R4H will measure the lift force and Bridge of R1V, R2V, R3V and R4V will measure the drag force.

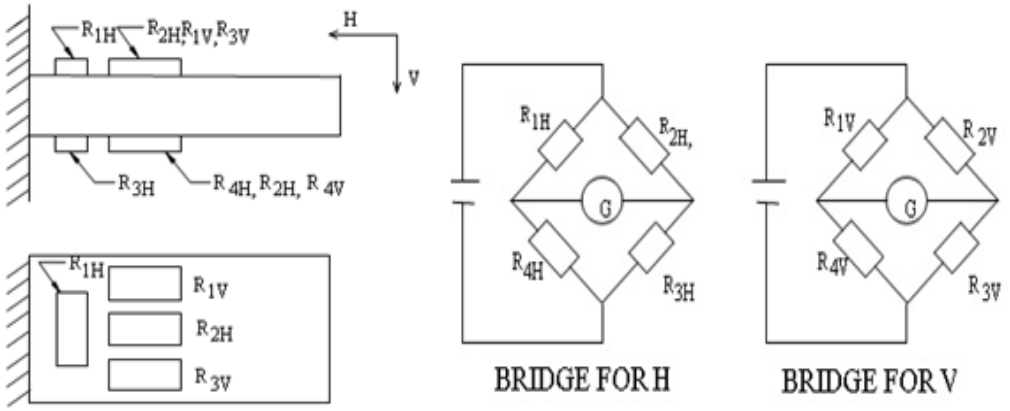

Fig. 3: Configuration and Circuit Diagrams for Strain Gauge Mounting and Usage.

The drag force (F_D) is given as

$$F_D = \frac{\in E \times BD^2}{24L} \tag{9}$$

Where B= width of beam, D= depth of beam and L= length of beam used for strain gauge shown in Figure 3.

And Lift force (F_L) is given as

$$F_L = \frac{\in (B \times D \times E)}{2.6} \tag{10}$$

3. WIND TUNNEL TESTING

The wind tunnel test was carried out in the Fluid Mechanics Laboratory of Department of Mechanical Engineering Jamia Millia Islamia, New Delhi. Its sketch is shown in Figure 4.

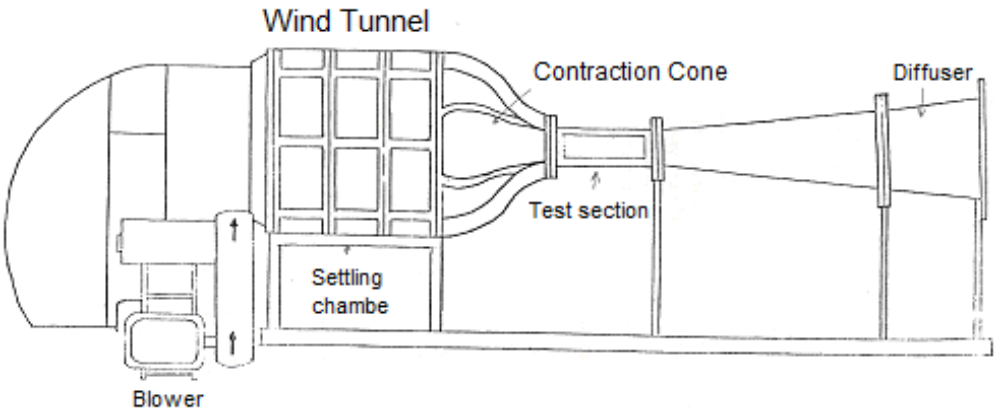

Fig. 4: Sketch of Wind Tunnel.

3.1. Description of various sections of wind tunnel

A wind tunnel is required to blow a jet of air or the body of vehicle. Various types of tunnels can be used for vehicle testing depending on the type and range of information required.

a) Source and capacity of air: Heavy duty centrifugal blower to generate air at test section with velocity of 9.6 m/s to 30 m/s. Using heavy duty motor Inlet Control a valve will be provided in blower for varying air flow velocity. The blower can be either of the axial or centrifugal type. In the axial type the driving motor can either be kept in the entry duct or outside it. In a large blower the electric motor is more conveniently kept on the floor. It drives the blower through step-up pulleys and belts. This avoids heating up of the entering air and does not restrict the passages of air through the entry duct.

b) Wide-angle diffuser: Wide-angle diffuser will be suitable to accept the out flow from the blower and deliver it to the setting chamber. For change of cross section from

blower and setting chamber, the duct is made from mild steel. The air from the blower is supplied to the settling chamber through a short diffuser. It is more economical and practical to allow an expansion of flow from the diffuser exit to the large settling chamber than to provide a long diffuser of a large area ratio. On account of large cross-sectional area of the settling chamber, the flow velocity is reduced to a small value. This and the presence of wire gauzes and honey combs straighten the flow before it is expanded in the contraction cone.

c) Setting chamber with flow distribution system: Honey combs and bank of screens to be fitted in the setting chamber with suitable flexible, fixture.

d) Contraction: The change of cross section from that of the setting chamber to the test section for monotonic. Distribution and uniformity of flow, design is based on modified Waite's method with L/D ratio of 1 to 1:5. The exit of the contraction cone is rectangular or square. Both pairs of contraction walls may or the contraction may be achieved in two stages, i.e. by converging the two pairs of walls separately in two stages. This arrangement gives a large overall length. The profiles of the converging walls must be carefully designed to avoid separation and thickening of the boundary layers.

e) Test section: This section receive flow contraction side arrangement with transparent windows and removable Top and Bottom Panel for fixing models and pressure probes size 300 mm x 300 mm of length about 1 meter. The test section receives a uniform stream of air from the contraction. The exit of the test section is oblique, i.e. its top and bottom walls are unequal to receive the inclined surface of the vehicle.

f) Exhaust section: Duct with downstream diffuser handling the exit flow from the tunnel for discharges to atmosphere, length, shape, and configuration to suit the test section and maximum velocity.

3.2 Operation of Wind Tunnel

a) Ensure that the three phase 400 V-50 c/s power is connected to the blower motor through 3-phase switch.

b) Ensure that the flow control valve of the blower is fully closed so that the motor is started without any air flow input.

c) Start the blower motor.

d) By slowly adjusting the input flow control valves of blower the flow velocity can be adjusted to desired flow rate.

e) Depending on the study experimental models which is installed in the test section, their behavior against flow can be studies using strain indicator.

5. EXPERIMENTAL

Experimental setup for testing is shown in Figure 5.

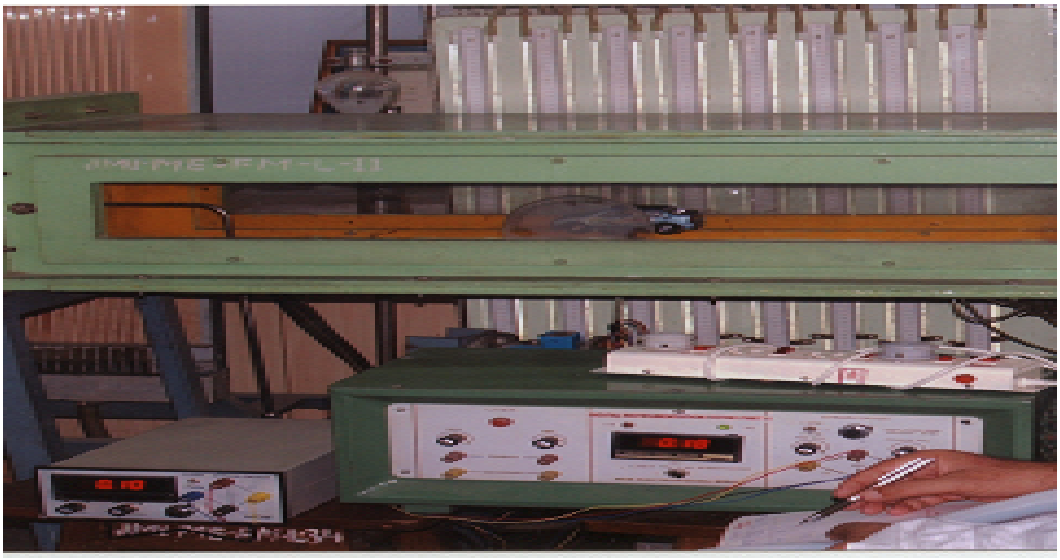

Fig. 5: Testing of Maruti Esteem Car on Wind Tunnel.

5. RESULTS AND DISCUSSIONS

On the basis of our experimental computation, we have to analyze results through tabular and graphical study. We summarized the results in the following sections.

5.1. Experimental Drag Force for Maruti Esteem Car at Different Velocities

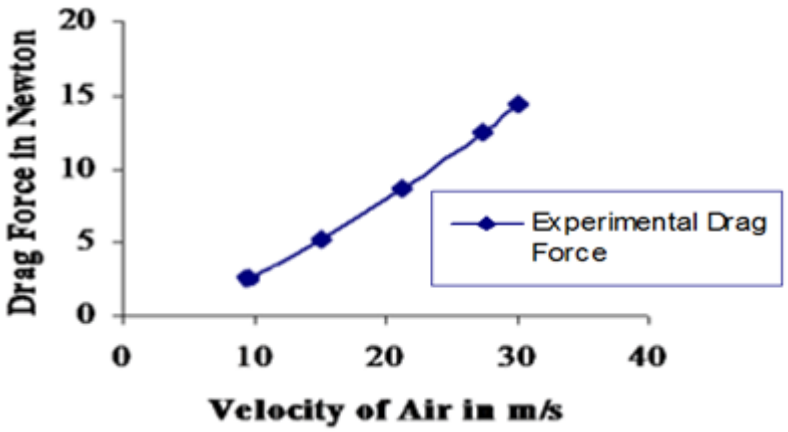

Fig. 6: Relation between Experimental Drag force and Velocity of Air.

In Table 1, Figure 6, we also depict the variation of experimental drag force with respect to air velocity. The trend of the graph is increasing in nature and drag force increases with velocity of air of the vehicle. Therefore drag force is the function of velocity of air at higher velocity the drag force is more and at lower velocity it is low.

Table 1: Experimental Drag Force for Maruti Esteem Car at Different Velocities.

S. No.	Velocity of air, u_0, in m/s	Experimental drag force in Newton
1.	9.6	2.6
2.	15.21	5.18
3.	21.21	8.72
4.	27.27	12.44
5.	30.00	14.40

5.2. Variation of Co-efficient of Drag Force with Velocity of Air for Maruti Esteem Car

Table 2: Variation of Co-efficient of Drag Force with Velocity of Air for Maruti Esteem Car.

S. No.	Velocity of air, u_0, m/s	Coefficient drag at Bonnet portion, C_d	Coefficient drag at Roof portion, C_d	Coefficient drag at windscreen portion, C_d
1.	9.6	8.8×10^{-3}	8.3×10^{-3}	6.62×10^{-3}
2.	15.21	7.024×10^{-3}	6.48×10^{-3}	5.27×10^{-3}
3.	21.21	5.9×10^{-3}	5.5×10^{-3}	4.48×10^{-3}
4.	27.27	5.23×10^{-3}	4.8×10^{-3}	3.9×10^{-3}
5.	30.00	4.99×10^{-3}	4.6×10^{-3}	3.76×10^{-3}

Sections of the car like bonnet, roof and wind screen with air velocity, the coefficient of drag is a function of velocity and increases with increasing the velocity of vehicle. The coefficient of drag is higher for lower velocity. Table 2 and Figure 7, shows the variation of coefficient of drag force at various velocities for different parts. It is greatest for the bonnet portions and lower for wind screen at all velocities.

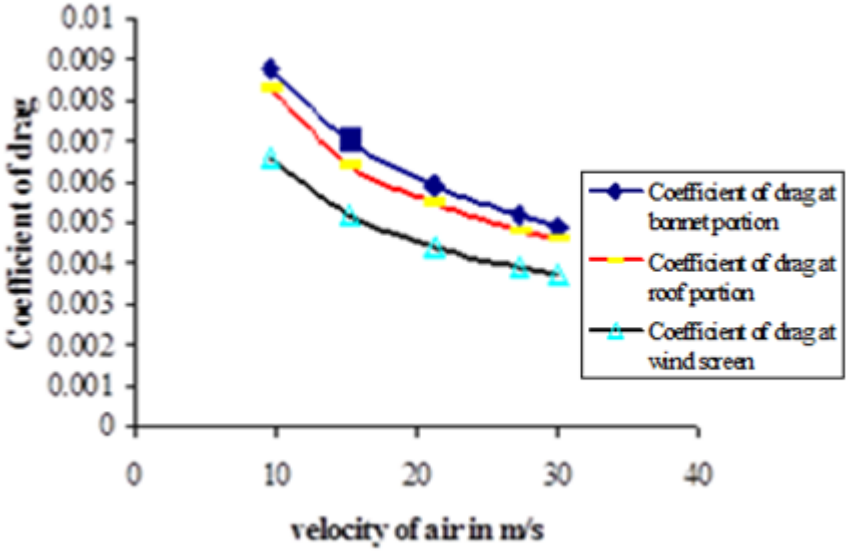

Fig. 7: Variation of Co-efficient of Drag Force with Velocity of Air for Maruti Esteem Car.

5.3. Variation of Reynolds Number with Velocity of Air for Maruti Esteem

Table 3: Variation of Reynolds Number with Velocity of Air for Maruti Esteem

S. No.	Velocity of air, u_0, in m/s	Reynolds No. at Bonnet portion	Reynolds No. at Roof portion	Reynolds No. at Wind screen
1.	9.6	838	905	739
2.	15.21	1055	1140	930
3.	21.21	1246	1345	1098
4.	27.27	1413	1525	1245
5.	30.00	1640	1720	1435

Table 3 and Figure 8, shows the variation of Reynolds number with velocity of air. We observe that Reynolds Number increases with the velocity of air. Again we get a higher Reynolds Number for bonnet, roof and wind screen portion as velocity increases.

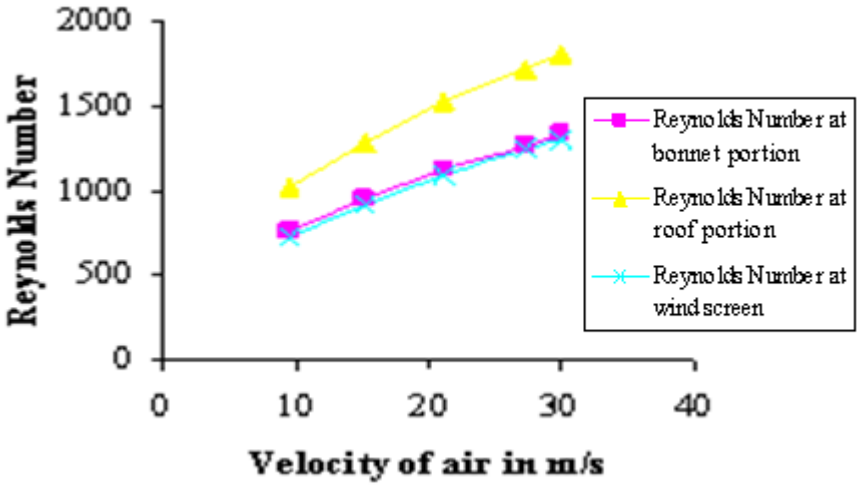

Fig. 8: Variation of Reynolds Number with Velocity of Air for Maruti Esteem.

6. CONCLUSION

The resistance to motion of car is offered by air and ground. In this investigation only air resistance has been chosen. The air resistance in the direction of motion of the car has been identified as drag. Theoretically we have considered a plate obstructing the flow of air. The theoretical considerations were confined to an obstructed flow up to the inclined plate and experimentally we found the drag force on a car model having a fixed inclination of windscreen. The windscreen in actual car as well as in car models represented the inclined plate obstructing the flow. Different car models used in experiment represented the inclined plate at fixed angle. Thus each model had only air velocity as variable. Yet it is to be understood well that the experimental value of resistance is more likely to exceed the theoretically computed value, because the area over which drag occur is larger than the area of the windscreen. The air flows over the bonnet and breaks on the sides of the car. The bonnet is more closed to the horizontal and sides are parallel to flow though not exactly. Both the bonnet surface and side surface as well as the roof may not offer great deal of drag but the corners where bonnet meets the wind screen, wind screen meets the sides and roof are the sources of increased drag. In theoretical consideration these effects were not taken into consideration.

The Figure 6, 7 and 8 represents the results for Maruti Esteem car model. The windscreen in the model is inclined to vertical at 60^0. Theoretically and experimentally results are similar in nature. At each velocity the experimental drag force exceed the theoretical drag force by about 35% of the theoretical drag force. The Maruti Esteem has fairly larger length of almost horizontal bonnet portion and experimental drag force has to be combined effects of inclined windscreen and horizontal bonnet.

This lead to the idea in designing shapes of the car body that designer is not restricted to make the bonnet much inclined as is seen in most cars these days. The designers should only concentrate on inclination of windscreen.

REFERENCES

[1] C.P. van Dam; "Recent experiences with different methods of drag prediction", Progr. Aerospace Sci., Vol. 35(8), pp. 751-798, 1999.

[2] E. Laurent; "Aerodynamique automobile", Mecanique & Industries, Vol. 2(3), pp.199-210, 2001.

[3] M. Gad-el-Haq; "Complaint coating for drag reduction", Progr. Aerospace Sci., Vol. 38(1), pp.77-99, 2002.

[4] D. Nixon; "A relationship between wave drag and induced drag", World Aviation Congr. Expo. (Session Aerodyn.), Montreal, QC, Canada, September, 2003.

[5] D. Destarac and J. van der Vooren; "Drag/thrust analysis of jet propelled transonic transport aircraft: definition of physical drag component", Aerospace Sci. Technol., Vol. 8(6), pp. 545-556, 2004.

[6] J.M. Zhan, X.P. Jia, Y.S. Li, M.G. Sun, G.X. Guo and Y.Z. Hu; "Analytical and experimental investigation of drag on nets of fish cages", Aquaculture. Engng, Vol. 35(1), pp. 91-101, 2006.

[7] D. Palaniappan and H. Ramkissoon; "A Drag Formula Revisited", Int. J. Engg. Sci., Vol. 43(19-20), pp. 1948-1501, 2005.

[8] Y. Shao and Y. Yang; "A scheme for drag partition over rough surfaces", Atmospheric Environment, Vol. 39(38), pp. 7351-7364, 2005.

[9] M. Kumar and V.A. Subramanian; "A numerical and experimental study on tank wall influences in drag estimation", Ocean Engg., Vol. 34(1), pp. 192-205, 2006.

AUTHOR'S BIOGRAPHY

Currently author is working in Department of Mechanical and Industrial Engineering, Majmaah University, K.S.A. His research is going on a new topic heat recovery from vehicle exhaust gas and utilizes it to vapor absorption air-conditioning purposes. His research fields of activities include boundary layer drag estimation on the body of automobiles. He has more than twenty-two research publications in journals at national and international levels. He has guided four Ph.D theses as co guide and thirteen M.Tech projects and written a book on Mechanical automation in 2012-13. His mail is vakkarali@yahoo.com